HIGH TEMPERATURE FATIGUE OF 304 STAINLESS STEEL UNDER ISOTHERMAL AND THERMAL CYCLING CONDITIONS

H. J. Westwood*

INTRODUCTION

In regions of stress concentration, many components of electrical generating plant experience low-cycle fatigue during start-up, shut-down periods, and creep under steady state loading conditions. The mechanical strain cycle is usually associated with a temperature cycle so that laboratory tests of fatigue resistance under simulated operational conditions should ideally incorporate combined thermal-mechanical cycling together with a hold time at maximum temperature. Most fatigue work, however, has been performed isothermally at the maximum operational temperature. In justifying this approach, it is often claimed that superimposition of a thermal cycle does not affect the fatigue life. Some recent studies, however, have shown that isothermal fatigue life can sometimes seriously overestimate the life under thermal cycling conditions [1, 2, 3].

This paper reports some results on type 304 stainless steel tested under two kinds of combined thermal-mechanical cycle, and also under isothermal conditions. Fatigue life Nf has been determined as a function of plastic strain range $\Delta\varepsilon p$, and metallographic studies of the damage mechanisms have been made.

EXPERIMENTAL

Test Rig

Tests were performed on an Instron Model 1115M fitted with suitable grips for reverse stress low cycle fatigue testing. The specimen was of the conventional hour-glass configuration having a gauge length of 20 mm and diameter 9.53 mm. A hollow gauge length was used in order to minimize radial temperature gradients, the internal diameter being 5.16 mm.

Heating of the specimen was by direct resistance which necessitated electrically isolating the grips from the rest of the machine. Temperature cycles were controlled by a Data-Track programmer which was also used to synchronize the mechanical and thermal cycles by stopping or reversing the Instron cross-head at appropriate points on the temperature programme. The mechanical strain range was varied by using different combinations of cross-head speed and transient times. In all tests the hold time was kept constant.

*W. P. Dobson Research Laboratory, Ontario Hydro, Kipling Avenue, Toronto, Ontario, Canada.

MATERIAL AND HEAT TREATMENT

Specimens were machined from type 304 stainless bar stock and were given the following heat treatment before test in order to stabilize the microstructure as far as possible:

(i) 1/2h at 1323 K, air cool
(ii) 2 h at 998 K, air cool

TEST CYCLES

The three types of tests are shown schematically in Figure 1. Modes I and II tests involve combined thermal-mechanical cycling, the former having maximum tensile strain at maximum temperature, the latter maximum compressive strain at maximum temperature. The temperature cycle was between 623 - 973 K, the Isothermal tests being performed at the latter temperature.

FATIGUE LOOPS

Figure 2 shows schematic representations of the kind of fatigue loops resulting from the three kinds of test. In the Isothermal case, the loop is more-or-less symmetrical with roughly equal maximum tensile and compressive stresses. The Modes I and II loops are less symmetrical, higher stress being reached at the lower temperature of the cycle, as a consequence of the flow-stress temperature dependency. For the same reason, maximum stress in the high temperature part of the cycle occurs at an intermediate temperature rather than at the maximum.

DETERMINATION OF STRAIN VALUES FROM FATIGUE LOOPS

Because of technical difficulties inherent in the use of high temperature extensometry, it was decided to determine the strain values after test from the load vs extension chart produced by the Instron. Figure 3 shows a representative chart, in this case from an Isothermal test. Several corrections are required in order to obtain the total strain $2\Delta\varepsilon t$ and total plastic strain $2\Delta\varepsilon p$ from such loops. Firstly, in all tests, the elastic strain component includes the elastic deflection of the machine and grips. Secondly, in Modes I and II tests, part of the strain is due to thermal expansion or contraction. In Mode I tests, this thermal strain must be deducted from the apparent strain whilst, in Mode II tests, it is added. This correction is required since it is only the mechanical strain in excess of the thermal strain which would result from unrestrained expansion and contraction, which produces fatigue damage in thermal cycling tests.

ELASTIC STRAIN CORRECTION

The elastic correction was determined by summing the deflections resulting from the maximum tensile and compressive loads, as given by a calibration curve of load train deflection vs load. In Mode I tests the maximum tensile load was taken as the load at the start of the hold time. Similarly, for Mode II tests, the maximum compressive load was taken at this point.

THERMAL STRAIN CORRECTION

To compensate for thermal strains in Modes I and II tests, an effective cross-head rate was utilized where:

$$\text{Effective cross-head rate} = \text{applied cross-head rate} - \text{thermal rate (Mode I)} \quad (1)$$

or

$$\text{Effective cross-head rate} = \text{applied cross-head rate} + \text{thermal rate (Mode II)} \quad (2)$$

The thermal rate was given by:

$$\text{Thermal rate} = \text{thermal strain} \div \text{transient time.} \quad (3)$$

The thermal strain was determined by measuring the free expansion and contraction of the specimen and grips during a thermal cycle.

DETERMINATION OF TOTAL STRAIN AND PLASTIC STRAIN

Referring to the loop in Figure 3, the horizontal axis can be read directly in time, since for all tests, a chart speed of 1 cm/min was used. Total and plastic strains $2\Delta\varepsilon t$ and $2\Delta\varepsilon p$ were determined from the following equations:

$$2\Delta\varepsilon t = \left\{\frac{(AB \times \text{effective rate}) - \text{elastic correction}}{\text{gauge length}}\right\} \times 100\% \quad (4)$$

$$2\Delta\varepsilon p = \left\{\frac{CD \times \text{effective rate}}{\text{gauge length}}\right\} 100\% \quad (5)$$

FAILURE CRITERION

This was taken as the number of cycles, Nf, at which complete fracture of the specimen occurred.

RESULTS AND DISCUSSION

Fatigue LIfe vs % Plastic Strain

Table 1 presents complete data for all the tests. Figure 4 shows fatigue life Nf as a function of plastic strain range $\Delta\varepsilon p$ for the three types of test. Included in the Isothermal results is the result of a tensile test in which fracture can be regarded as occurring in 0.25 fatigue cycles. In choosing the best straight lines to represent the Modes I and II results, an assumption was made that the results should extrapolate back to predict the same tensile ductility as in the Isothermal tests. Although Mode I fractures occurred near to 973 K whilst Mode II were nearer to 623 K, the tensile ductility of 304 does not differ widely at these temperature extremes [4]. In the Mode II results the two points corresponding to Nf values of 2.25 and 6 were deliberately excluded from the line because the specimens buckled during test. Thus the axial strains would have been less than the calculated values.

Coffin [5] and Manson [6] both proposed the following equation relating plastic strain range $\Delta\varepsilon p$ to low-cycle fatigue life Nf:

$$\Delta\varepsilon p = C\ Nf^{-B} \tag{6}$$

where C and B are constants. The lines drawn in Figure 2 satisfy the following equations:

$$\text{Mode I} \qquad \Delta\varepsilon p = 0.14\ Nf^{-0.67} \tag{7}$$

$$\text{Mode II} \qquad \Delta\varepsilon p = 0.17\ Nf^{-0.55} \tag{8}$$

$$\text{Isothermal} \qquad \Delta\varepsilon p = 0.14\ Nf^{-0.73} \tag{9}$$

The main point emerging from these results is that, in the temperature and strain range examined, there is no significant difference in fatigue life under Mode I and Isothermal conditions, whilst the Mode II life is significantly greater. These results are in substantial agreement with those of Stentz, Berling and Conway [1]. These workers, however, also showed that in tests without hold times, the Mode I life was only about 1/3 of the Isothermal life.

Stability of Fatigue Loops

The fatigue loop shown in Figure 3 was typical of all those produced in Isothermal tests. In these, loops generated by successive fatigue cycles were superimposed on previous loops, indicating that fully reversed plastic strain was occurring. In the Modes I and II tests, such was not the case. Figure 5 shows a series of loops from a Mode I test. Each successive loop is slightly displaced from its predecessor showing that full plastic strain reversal was not occurring, or that ratchetting was taking place. In Mode I tests, the ratchetting was in the tensile direction, whereas compressive ratchetting occurred in Mode II tests.

Metallographic Examination

Figure 6 shows specimens after fracture in the three kinds of test, the Nf value being about 20 in each case. Several features are noteworthy: (i) in Mode I, fracture was preceded by necking, (ii) no necking occurred in the Isothermal specimen, (iii) bulging of the specimen occurred in Mode II with fracture occurring outside the bulged region.

The fractured specimens were sectioned longitudinally and prepared for metallographic examination. Note that the micrographs only show one side of the specimens since these were tubular in section.

The Mode I fracture was intergranular in nature and fairly profuse intergranular cavitation in the fracture region clearly indicated that linkage of cavities was the fracture mechanism. Typical cavitation damage is shown in Figure 7. Some surface cracking had also occurred but had not penetrated more than one or two grains.

The Mode II fracture mechanism involved growth of cracks from the surface. A typical crack, in this case from a specimen not taken to complete fracture, is shown in Figure 8. The crack path is clearly transgranular, fairly typical of low-cycle fatigue cracking at temperatures below the creep range. Final fracture in Mode II resulted from ductile rupture due

to tensile overload after surface cracking had penetrated roughly two thirds of the cross-section. Tensile strain is indicated by the width of the crack in Figure 8.

The Isothermal fracture also resulted from growth of surface cracks but, in this case, the crack path was essentially intergranular as shown in Figure 9. No significant cavitation damage was associated with the fracture which could be described as typical of high temperature low cycle fatigue.

Damage Mechanisms

The three distinct fracture mechanisms can be explained in terms of the stress-strain-temperature relationships, as indicated by the fatigue loops.

In the Isothermal tests, fully reversed plastic strain occurred and fracture resulted from growth of intergranular cracks from the surface. It is not certain whether the crack propagation mechanism involved creep damage, i.e. cavitation or grain boundary environmental attack. Growth of intergranular cavities involves vacancy condensation so that zero growth might be predicted under reverse stress cycling, growth in the tensile half-cycle being removed by sintering in the compressive half-cycle. Weertman has shown, however, that second order effects can allow some slow cavity growth under such conditions [7], and intergranular cavitation has been shown to initiate low cycle fatigue fracture, e.g. in copper alloys [8] and in iron at 973 K [9]. Comparative tests in air and vacuum, however, have led Coffin to the view that intergranular cracking in high temperature fatigue is mainly due to grain boundary oxidation [10]. In 304 stainless tested under vacuum, no intergranular cracking was found even in very low frequency tests at 923 K. This evidence, plus the absence of intergranular cavitation ahead of the crack tip, suggests that fracture in the Isothermal specimens was mainly due to environmental attack via the grain boundaries.

The Mode I fractures clearly resulted from intergranular cavitation and appeared to be directly associated with the ratchetting whereby an increment of tensile creep resulted from each fatigue cycle. The ratchetting was a consequence of the increased flow stress at the lower end of the temperature cycle which prevented complete plastic strain reversal. Limited evidence from interrupted tests indicated that fracture occurred within a few cycles of the cavitation becoming optically detectable. This suggests that growth of cavities to the extent of one grain facet may have been the controlling factor [11]. Subsequent propagation to a critical crack length appeared to be relatively easy.

The transgranular cracking in Mode II specimens reflects the fact that fracture took place at the low end of the temperature cycle where creep and or environmental effects would be less significant. The longer fatigue life in these specimens is also partly attributable to the lower temperature of fracture since it is well known that fatigue resistance decreases as temperature increases into the creep range. The Mode II fracture mechanism could be associated indirectly with the compressive ratchetting which caused the observed bulging in these specimens. Thus, each increment of compressive creep strain caused a corresponding tensile increment in the subsequent half-cycle, so that when cracks were growing, the net section stress would be increasing rapidly and effectively increasing the tensile strain range. This resulted in the observed widening of the fatigue cracks and led to eventual failure by tensile rupture.

CONCLUSIONS

1. In thermal cycling tests on 304 stainless, when the maximum tensile strain occured at maximum temperature, (Mode I) the fatigue life was the same as in isothermal tests at the same maximum temperature. When maximum compressive strain occurred at maximum temperature, (Mode II) longer fatigue lives resulted.

2. Damage and fracture mechanisms were different in the three tests. Mode I fractures resulted from intergranular cavitation, Mode II from transgranular surface cracking together with tensile rupture, and Isothermal from intergranular surface cracking.

REFERENCES

1. STENTZ, R. H., BERLING, J. T. and CONWAY, J. B., Proceedings International Conference on Structural Mechanics in Reactor Technology, Berlin, 1971.
2. LINDHOLM, U. S. and DAVIDSON, D. L., American Society for Testing and Materials, ASTM ST 520, 1973, 473.
3. SHEFFLER, K. D. and DOBLE, G. S., American Society for Testing and Materials, ASTM STP 520, 1973, 491.
4. ASTM Data Series Publication DS5-51, 9.
5. COFFIN, L. F., Jr., Trans ASME 76, 1954, 931.
6. MANSON, S. S., NACA Technical Note 2933, NASA Lewis Research Centre, Cleveland, Ohio, 1954.
7. WEERTMAN, J., Met. Trans. 5, 1974, 1743.
8. COLLINS, A. L. W., COCKS, G. J. and TAPLIN, D. M. R., Met. Sci. J. March, 1977.
9. WESTWOOD, H. J. and TAPLIN, D. M. R., Met. Trans. 3, 1972, 1959.
10. COFFIN, L. F., Jr., Fracture 1977 (ed. D. M. R. Taplin), University of Waterloo Press, Canada, 1977.
11. FLECK, R. G., BEEVERS, C. J. and TAPLIN, D. M. R., Met. Sci. J. 9, 1975, 49.

Table 1 Complete Test Data

Test No	Type	Transient min	Hold min	C/Head Rate cm/sec	Effective Rate cm/sec	AB min	CD min	Stress (t) MPa	Stress (C) MPa	Stress (R) MPa	Elastic Corr'n cm	Total Strain 2 εt %	Total Plastic Strain 2 εt %	Cycles to Failure Nf
104	Mode I	5.63	5.63	0.05	0.0447	5.50	4.40	126.8	351.0	-	0.026	11.0	9.8	3
101	"	8.40	5.40	0.02	0.0164	8.85	7.00	102.4	258.4	29.3	0.020	6.3	5.7	7.25
102	"	5.63	5.63	0.02	0.0147	5.40	3.80	112.1	229.1	29.3	0.020	3.0	2.8	14.5
105	"	7.38	5.47	0.01	0.0060	7.15	4.00	107.3	195.0	39.0	0.017	1.3	1.2	80
103	"	8.40	5.40	0.01	0.0064	8.20	4.30	112.1	185.3	48.8	0.017	1.8	1.4	108
121	Mode II	7.38	5.47	0.10	0.1040	7.30	6.60	487.5	312.0	97.5	0.043	35.8	34.3	2.25
118	"	8.40	5.40	0.05	0.0536	8.40	7.50	458.3	341.3	97.5	0.042	20.4	20.1	6
112	"	5.63	5.63	0.02	0.0253	5.40	4.00	319.8	234.0	117.0	0.040	4.8	5.1	18
119	"	8.40	5.40	0.02	0.0236	8.10	5.70	399.8	219.4	195.0	0.038	7.7	6.7	20
120	"	5.63	5.63	0.01	0.0153	5.40	3.20	224.3	165.8	165.8	0.027		2.5	149
106	Isothermal		5.63	0.05	0.05	5.60	4.50	87.8	209.6	19.5	0.018	13.1	11.3	3.25
108	"		5.40	0.01	0.01	8.40	6.00	136.5	144.3	85.8	0.016	3.4	3.0	19
109	"		5.47	0.01	0.01	7.20	5.00	97.5	136.5	48.8	0.014	2.9	2.5	26
110	"		5.63	0.005	0.005	5.45	1.40	87.8	139.2	58.5	0.011	0.8	0.4	233
111	Tensile			0.02				185.3					35.0	0.25

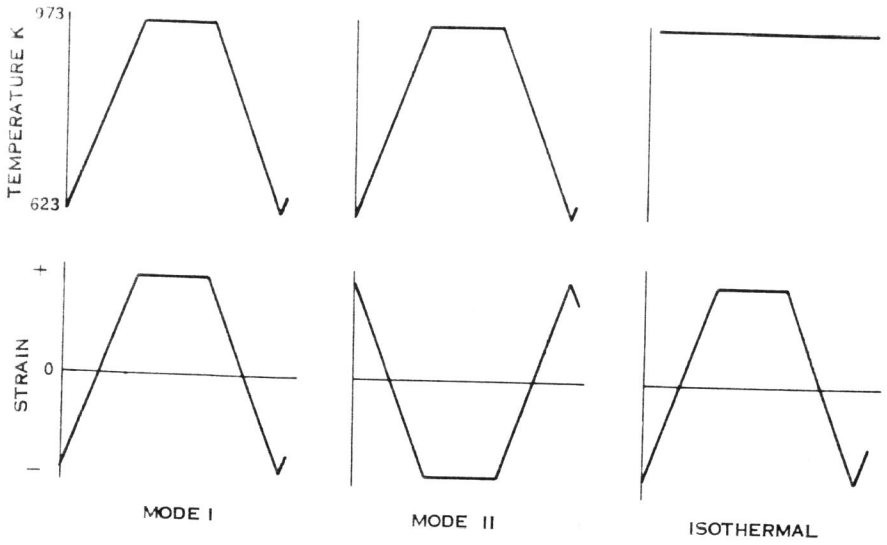

Figure 1 Temperature - Strain Relationships for the 3 Kinds of Test

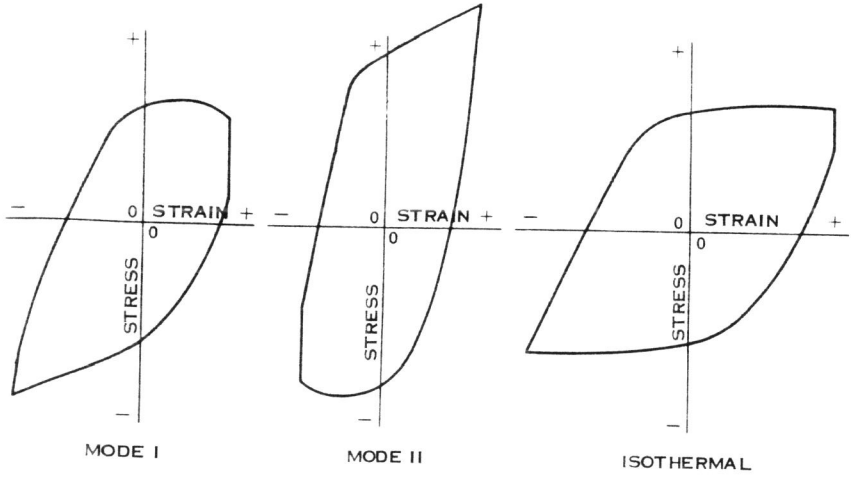

Figure 2 Schematic Representation of Fatigue Loops for the 3 Kinds of Test

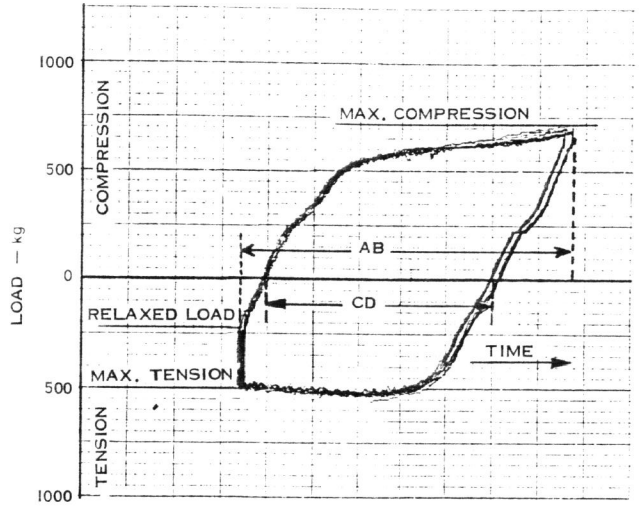

Figure 3 Representative Instron Chart - from an Isothermal Test

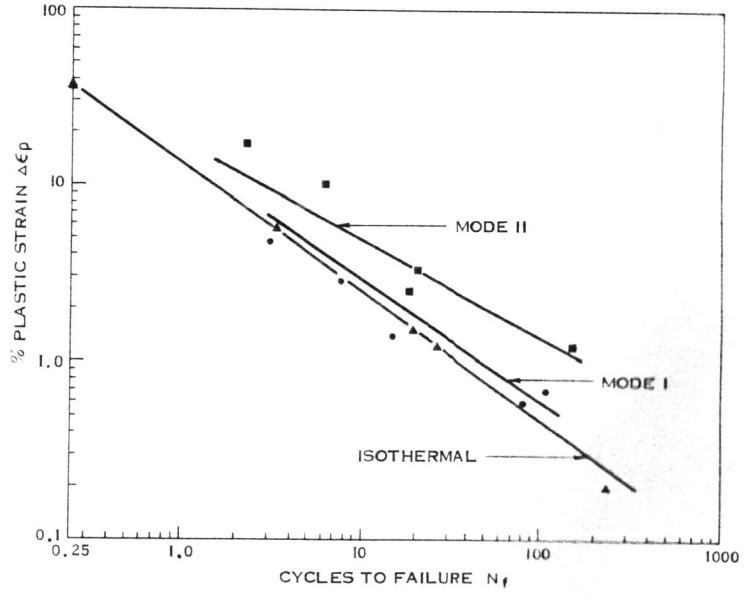

Figure 4 Fatigue Life N_f versus Plastic Strain $\Delta\varepsilon_p$ for the 3 Kinds of Test

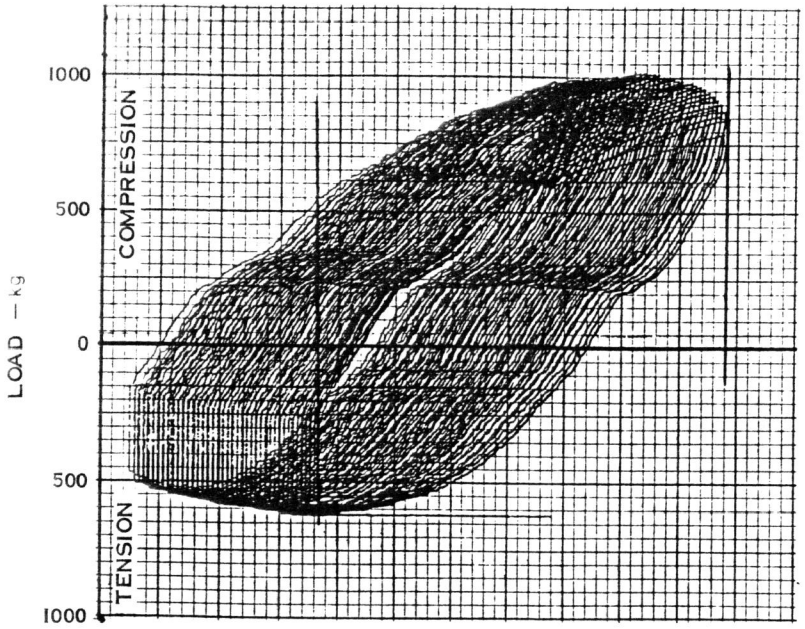

Figure 5 Tensile Ratchetting in Mode I Test

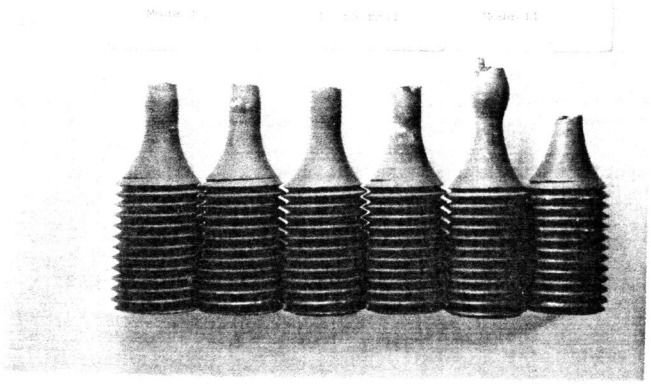

Figure 6 Specimens Fractured in the 3 Kinds of Test

Figure 7 Intergranular Cavitation Damage in Mode I Specimen

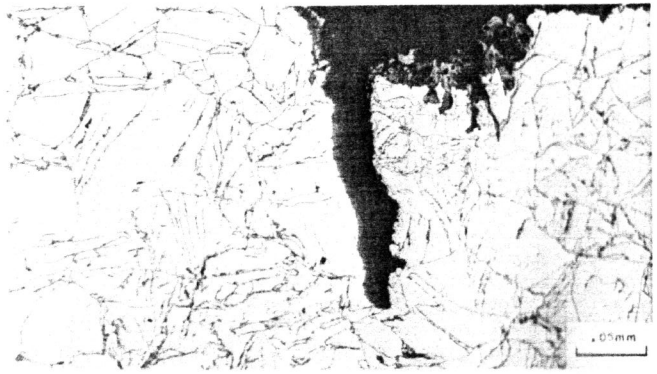

Figure 8 Transgranular Surface Crack in Mode II Specimen

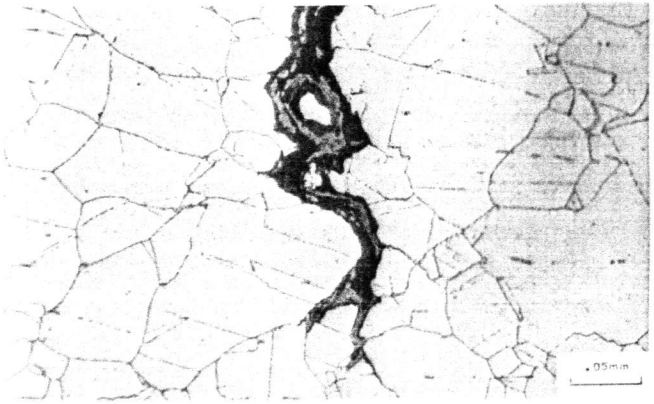

Figure 9 Intergranular Surface Crack in Isothermal Specimen